The Distance to the Soft Gamma Repeater SGR 1627–41.

S. Corbel[1], C. Chapuis[1], T.M. Dame[2] and P. Durouchoux[1]

Received ______________________; accepted ______________________

Accepted for publication in ApJ Letters

[1]Service d'Astrophysique, CEA Saclay, 91191 Gif sur Yvette Cedex, France

[2]Harvard Smithsonian Center for Astrophysics, 60 Garden Street, Cambridge, MA 02138, USA

ABSTRACT

We report millimeter observations of the line of sight to the recently discovered Soft Gamma Repeater, SGR 1627–41, which has been tentatively associated with the supernova remnant SNR G 337.0–0.1. Among the eight molecular clouds along the line of sight to SGR 1627–41, we show that SNR G 337.0–0.1 is probably interacting with one of the most massive giant molecular clouds (GMC) in the Galaxy, at a distance of 11 kpc from the sun. Based on the high extinction to the persistent X-ray counterpart of SGR 1627–41, we present evidence for an association of this new SGR with the SNR G 337.0–0.1; they both appear to be located on the near side of the GMC. This is the second SGR located near an extraordinarily massive GMC. We suggest that SGR 1627–41 is a neutron star with a high transverse velocity ($\sim$ 1,000 km s^{-1}) escaping the young ($\sim$ 5,000 years) supernova remnant G 337.0–0.1.

Subject headings: gamma rays: bursts — stars: individual (SGR 1627–41) — stars: neutron — ISM: individual (CTB 33, G 337.0–0.1)

1. Introduction

Soft Gamma Repeaters (SGRs) are believed to be young neutron stars of high dipolar magnetic field, located in or near their associated supernova remnants (SNRs). A key observation regarding the nature of these objects was the simultaneous detection by *ASCA* and *BATSE* of a burst from SGR 1806–20 (Kouveliotou et al. 1994, Murakami et al. 1994), which allowed an accurate determination of the burst position. Subsequent observations revealed a persistent X-ray counterpart, located near the center of the young plerionic SNR G 10.0–0.3 (Murakami et al. 1994, Sonobe et al. 1994, Kulkarni et al. 1994). Further insights into the nature of SGRs came from the detection by *RXTE* of a very slow pulsation (7.47 s) with a very high spin down from the persistent X-ray counterpart of SGR 1806–20, implying an extremely strong dipolar magnetic field (8×10^{14} Gauss) for the neutron star (Kouveliotou et al. 1998a). This results provided the first strong observational support for the magnetar model of Thomson & Duncan (1995), in which SGRs are young and strongly magnetized neutron stars. SGR 1806–20 is associated with a giant molecular cloud (GMC) at a distance of 14.5 kpc from the sun (Corbel et al. 1997). In 1998, an *ASCA* observation of SGR 1900+14 during a bursting phase (Murakami et al. 1999, Hurley et al. 1999a), provided an improved position, and revealed a persistent X-ray counterpart, similar to that of SGR 1806–20. *ASCA*, *RXTE* and *BeppoSAX* (Hurley et al. 1999a, Kouveliotou et al. 1999, Woods et al. 1999a) detected slow pulsation (5.16 s) from the persistent X-ray counterpart with a very high spin down, giving a dipolar magnetic field of $\sim 5 \times 10^{14}$ Gauss, again supporting the magnetar model.

SGR 1627–41 was discovered with *BATSE* (Kouveliotou et al. 1998b). Its accurate error box, combining measurements from *Ulysses*, *Konus-Wind*, *RXTE* and *BATSE* (Hurley et al. 1999b, Smith et al. 1999) contains the SNR G 337.0–0.1 (Woods et al. 1998). Observations with *BeppoSAX* revealed an X-ray source within the SNR, SAX J1635.8–4736,

with a non thermal X-ray spectrum (Woods et al. 1999b) and a possible pulsation at 6.41 s. Based on the similar properties with other SGRs, it is very likely that they have detected the persistent X-ray counterpart of SGR 1627–41.

The very high interstellar absorption for SGR 1627–41 (Woods et al. 1999b) prompted us to perform millimeter observations in order to determine the source of this extinction. Here, we report observations carried out with the SEST telescope, allowing the detection of 8 distinct molecular clouds along the line of sight to SGR 1627–41. We show that SGR 1627–41 and the SNR G 337.0–0.1 are both associated with an exceptionally massive GMC at a distance of 11 kpc. We also show that the total extinction along the 11 kpc to the SGR, derived from CO and 21 cm observations, is consistent with the foreground extinction derived for the X-ray counterpart. We then discuss the consequences of this distance on the nature of SGR 1627–41.

2. Observations

The observations were carried out with the 15 m Swedish – ESO Submillimeter Telescope (SEST) at La Silla, Chile, on 1999 May 20. We observed the central position reported by Woods et al. (1999b). We simultaneously observed two transitions: ^{12}CO(J=1–0) and ^{12}CO(J=2–1), at 115.27 and 230.54 GHz respectively; the J=2–1 line is shown in Figure 1 (solid line). The FWHM beamwidth of SEST is 45″ at 115.27 GHz and 23″ at 230.54 GHz. We observed in position switching mode, after checking in frequency switching mode that our OFF position ($\alpha(2000)$ = 16h30m02.0s, $\delta(2000) = -46°23'32''$) was free of emission. The back end was an acousto-optical spectrometer with a frequency bandwidth of 1 GHz and a velocity resolution of 1.8 km s^{-1} at 115.27 GHz and 0.9 km s^{-1} at 230.54 GHz. The system was calibrated with the chopper wheel method; regular observations of calibration sources show that the SEST calibration is stable to within a few percent. The

system temperature during the observations was $\sim$ 284 K at 115.27 GHz and $\sim$ 197 K at 230.54 GHz. We obtained the 21 cm HI spectra (dotted line in Figure 1) from the survey of neutral hydrogen in the southern Galaxy, observed by Kerr et al. (1986). The spectrum used for this study is an average of the two observed spectra closest to SGR 1627–41, at l = 337°, b = 0° and –0.25° (SGR 1627–41 is at l= 337.0° and b = –0.1°).

3. Results

As the velocity resolution is slightly better in the ^{12}CO(J=2–1) spectrum (Figure 1) than the ^{12}CO(J=1–0), we have used it to separate the various molecular clouds along the line of sight to SGR 1627–41. The extinction has been derived from the ^{12}CO(J=1–0) spectrum. A total of 8 clouds can be identified. We label each of them with the acronym MC and its associated velocity in Figure 1. It is well known that for gas in the inner Galaxy, there are two possible distances corresponding to each radial velocity. The parameters associated with each cloud are displayed in Table 1, using a circular model for the Galactic rotation (Fich et al. 1989).

As we are primarily interested in the distribution of extinction along the line of sight, we have estimated the atomic hydrogen column density, taking into account opacity effect, by using the following relation (Rohlfs & Wilson 1996): $\frac{\mathcal{N}(\mathrm{H\ I})}{\mathrm{atome\ cm^{-2}}} = -1.82 \times 10^{18} \left(\frac{T_S}{\mathrm{K}}\right) \int \ln\left(1 - \frac{T_b(v)}{T_S - T_{bg}}\right) \frac{dv}{\mathrm{km\ s^{-1}}}$, and taking the usual assumption of T_S = 125 K for the spin temperature and T_{bg} = 2.7 K for the cosmic background temperature; T_b is the 21 cm line brightness temperature. Molecular hydrogen column density, N(H_2), was derived from velocity integrated ^{12}CO(J=1–0) intensity, W(CO), using a conversion factor, $X_{CO} \equiv$ N(H_2)/W(CO), of $(1.9 \pm 0.2) \times 10^{20}$ mols. cm^{-2}/(K km s^{-1}). This value was determined by comparing the γ-ray, HI and ^{12}CO(J=1–0) emissions from the Galaxy (Strong & Mattox, 1996). The ^{12}CO(J=1–0) transition has been shown to be the

best tracer of molecular cloud masses (Combes 1991), and three different methods have led to a similar value for X_{CO} (Solomon & Barrett 1991). The total hydrogen column density, N(H), is then N(H) = N(HI) + 2 N(H_2). We can estimate the total extinction using the following relation (Predehl & Schmitt 1995): $A_v = (5.6 \pm 0.1) \times 10^{-22} \times \mathcal{N}(H)$. Table 2 gives the extinction for each of the molecular clouds.

4. The supernova remnant G 337.0–0.1

In the MOST supernova remnant catalog (Whiteoak & Green 1996), G 337.0–0.1 has a non thermal spectrum and a peculiar morphology, with several intensity enhancements superposed on a plateau of emission. It is a member of the CTB 33 complex, which also includes the H II regions G 337.1–0.2 and G 336.8+0.0. Using high resolution radio observations, Sarma et al. (1997) clearly resolved the G 337.0–0.1 area into three components: another H II region, the supernova remnant G 337.0–0.1 and an edge source. Frail et al. (1996) detected a maser OH emission line from the SNR, G 337.0–0.1, at –71.3 km s^{-1}. As mentioned by Sarma et al. (1997), this OH line is in agreement with the velocity (–73 to –75 km s^{-1}) of the recombination lines from the H II regions of the CTB 33 complex. The HI absorption profiles (Sarma et al. 1997) toward the members of the CTB 33 complex (including the SNR G 337.0–0.1) show absorption features up to the tangent point, therefore ruling out the near distance. Based on the rotation curve model of Fich et al. (1989), a distance of 11.0 ± 0.3 kpc is deduced for the CTB 33 complex, including the SNR G 337.0–0.1 (Sarma et al. 1997).

In the ^{12}CO(J=2–1) spectrum toward SGR 1627–41 (Figure 1), which encompasses the direction of G 337.0–0.1, a GMC is detected at –70.9 km s^{-1}, close to the velocity of the components of the CTB 33 complex. In order to image the molecular emission in the vicinity of MC–71, we used the CO survey of Bronfman et al. (1989). The CO map in

Figure 2 is integrated over the velocity range –80 to –40 km s^{-1}, which includes all of the emission from MC–71 as well as that from an adjacent cloud at a velocity of –56 km s^{-1} (MC–56) which may be related (see below).

The coincidence of MC–71 in direction and velocity with both the H II regions G 337.1–0.2 and G 336.8+0.0 and the SNR G 337.0–0.1 strongly suggests that MC–71 is the progenitor of the entire CTB 33 complex, which lies at the far kinematic distance of 11 kpc. The radius-linewidth relation for GMCs (Dame et al. 1986) also favors the far kinematic distance for MC–71: this GMC has an exceptionally large composite linewidth of $\sim$ 19 km s^{-1} but a relatively small angular radius of $\sim 0.35°$, corresponding to 28 pc at the near kinematic distance of 4.7 kpc or a more appropriate 67 pc at the far distance. At the far distance, the CO luminosity of MC–71 implies a total molecular mass of 4×10^6 M$_\odot$, about the same as that of the GMC associated with SGR 1806–20 (Corbel et al. 1997) and comparable to the masses of the half dozen or so largest GMCs in the Galaxy (Dame et al. 1986; Solomon et al. 1987).

It is worth noting that MC–71 lies within $\sim 0.5°$ and $\sim$ 15 km s^{-1} of another GMC with very similar observational properties (size, mass). As Figure 2 shows, the GMC labeled MC–56 has about the same angular size as MC–71, and its composite linewidth is even larger than that of MC–71; therefore the far kinematic distance is again strongly favored by the radius-linewidth relation. Both these clouds coincide with a remarkable cluster of H II regions discussed by Mezger et al. (1970 – see especially their Fig. 2); they note that the cluster is very restricted in longitude but has a wide velocity spread (from $\sim$ −90 to –30 km s^{-1}). It is possible that the abundance of star formation associated with these two GMCs, including SGR 1627–41, may have resulted from their collision or tidal interaction.

The detection of the MC–71 molecular cloud gives a natural explanation for the hydroxyl radical (OH) maser detection from SNR G 337.0–0.1 by Frail et al. (1996). As

these authors pointed out, this maser line is collisionaly excited by the supernova remnant shock going through a molecular cloud. We note that our distance measurement of 11.0 ± 0.3 kpc for SNR G 337.0–0.1 is not consistent with the value of 5.8 kpc derived by Case & Bhattacharya (1998) using a new statistical Σ–D relation.

5. Distance and nature of SGR 1627–41

The total hydrogen column density toward the persistent X-ray counterpart of SGR 1627–41 is estimated to be $(7.7 \pm 0.8) \times 10^{22}$ cm^{-2} (Woods et al. 1999b). Using the empirical relation of Predehl & Schmitt (1995), this corresponds to an optical extinction of 43.0 ± 3.9 magnitudes. As the SNR G 337.0–0.1 is probably at a distance of 11.0 kpc and associated with MC–71, we will estimate the extinction up to the MC–71 cloud. The contribution of each cloud to the extinction is presented in Table 2. We note that the intrinsic extinction of MC–71 is very high ($\sim$ 40 magnitudes). The five molecular clouds with velocity lower than that of MC–71 (MC–122, MC–117, MC–110, MC–97 and MC–83) must be located in front of it, since both the near and far kinematic distances of these clouds are smaller than the distance of MC–71. The two clouds at higher velocity, MC–41 and MC–32, are apparently also in front of MC–71, at their near kinematic distances, since hydrogen absorption lines at the velocities of these clouds are seen against the radio continuum of the SNR G 337.0–0.1 (Sarma et al. 1997).

Summing the contributions from all the molecular clouds in front of MC–71 yields a total optical extinction of 30.0 ± 1.9 magnitudes. Contribution to the extinction from atomic hydrogen can be estimated as follows. Integrating all HI emission from –150 km s^{-1} to 0 km s^{-1} gives an upper limit of 11.4 magnitudes. It is possible that part of the HI emission from –71 km s^{-1} to 0 km s^{-1} arises from gas beyond MC–71; by assuming that half of this HI emission is at the near distance and the other half at the far distance, we

can deduce a lower limit of 8.0 magnitudes. Therefore, atomic hydrogen adds another 9.7 $\pm$ 1.7 magnitudes, giving a total extinction to MC–71 of 39.7 $\pm$ 2.5 magnitudes, in good agreement with the value 43.0 $\pm$ 3.9 mag. determined for the X-ray counterpart. Since MC–71 itself would increase the total extinction to 81.1 $\pm$ 4.5 magnitudes, a factor of two above the value derived for SAX J1635.8–4736, SGR 1627–41 must be located on the near side of MC–71. The distance to this cloud is obviously the same as that of the CTB 33 complex, i.e. SGR 1627–41 is at distance from the sun of 11.0 $\pm$ 0.3 kpc. This constitutes the second accurate distance estimate of a SGR. We should note that the other SGR for which a reasonable distance estimate exists – SGR 1806–20 at 14.5 $\pm$ 1.4 kpc (Corbel et al. 1997) – is also on the edge of a very massive GMC. This might indicate that these objects are still lying close to their birth sites.

The first detailed observations of G 337.0–0.1 by MOST (Whiteoak & Green 1996) showed a complex morphology which, as mentioned above, has been resolved into various components by Sarma et al. (1997). Their observations clearly revealed the intrinsic morphology of this supernova remnant (Fig. 3 in Sarma et al. (1997)), and therefore provides the best available radio map of G 337.0–0.1. Therefore, the SNR map of Sarma et al. (1997) is more appropriate for the study of G 337.0–0.1 than the much more widely used MOST map.

The angular size (radius of $\sim 45''$) of SNR G 337.0–0.1 implies a radius of 2.4 pc at a distance of 11.0 kpc. Following Kafatos et al. (1980), who have studied the expansion of SNRs in various environments, the size of G 337.0–0.1 is not in agreement with an expansion into a molecular cloud but is rather typical of a very young SNR ($<$ 1,000 years) expanding into the interstellar medium. This is consistent with our conclusion that G 337.0–0.1 is on the outer edge of MC–71 and with the fact that SGRs are believed to be associated with young SNR.

The persistent X-ray counterpart (the center of its associated error box (Hurley et al. 1999b)) is located $105 \pm 26\,''$ away from the projected center of the SNR G 337.0–0.1, which corresponds to a displacement of 5.4 pc with our distance estimate of SGR 1627–41. A very young SNR with an age of 1,000 years would require an unrealistic transverse velocity of 5,400 $\pm$ 1,300 km s^{-1} to reach this displacement, while a $\sim$ 5,000 years old SNR would imply a more reasonable velocity of 1,080 $\pm$ 270 km s^{-1} (requiring the expansion of the SNR into a *rarefied* interstellar medium). The latter number seems more likely as high velocity neutron stars have been found with transverse velocities up to $\sim$ 1,000 km s^{-1} (Harrison et al. 1993). Therefore it is possible that SGR 1627–41 is a high velocity neutron star escaping the young SNR G 337.0–0.1. These numbers could be refined with an improved position of the X-ray counterpart.

6. Conclusions

SGR 1627–41 is found to be located on the edge of a very massive GMC at a distance of 11.0 $\pm$ 0.3 kpc, with an optical extinction of $\sim$ 43 magnitudes. This is the second SGR located on the outer edge of a very large and massive GMC. We present evidence for an association with the supernova remnant G 337.0–0.1, which is interacting with the GMC. The position of SGR 1627–41 relative to the SNR indicates that SGR 1627–41 is probably escaping the young ($\sim$ 5,000 years) supernova remnant G 337.0–0.1 with a high transverse velocity ($\sim$ 1,000 km s^{-1}).

S.C. would like to thank I. Grenier for useful discussions on the X_{CO} factor. This research has made use of the SIMBAD database, operated at CDS, Strasbourg, France, and of the Astronomical Data Center (ADC) at NASA Goddard Space Flight Center.

REFERENCES

Bronfman, L., Alvarez, H., Cohen, R.S. & Thaddeus, P. 1989, ApJS, 71, 481

Case G.L. & Bhattacharya D. 1998, ApJ, 504, 761

Combes, F. 1991, ARA&A, 29, 195

Condon, J.J., Griffith, M.R. & Wright, A.E. 1993, AJ, 106, 1095

Corbel, S., Wallyn, P., Dame, T.M., Durouchoux, P., Mahoney, W.A., Vilhu, O. & Grindlay, J.E. 1997, ApJ, 478, 624

Dame, T.B., Elmegreen, B.G., Cohen, R.S. & Thaddeus, P. 1986, ApJ, 305, 892

Fich, M., Blitz, L. & Stark, A. 1989, ApJ, 342, 272

Frail, D.A., Goss, W.M., Reynoso, E.M., Giacani, E.B., Green, A.J. & Otrupcek, R. 1996, AJ, 111, 1651

Harrison, P.A., Lyne, A.G. & Anderson, B. 1993, MNRAS, 261, 113

Hurley, K. et al. 1999a, ApJ, 510, L111

Hurley, K., Kouveliotou, C., Woods, P., Mazets, E., Golenetskii, S.V., Fredericks, D.D., Cline, T. & van Paradijs, J. 1999b, ApJ, 519, L143

Kafatos, M., Sofia, S., Bruhweiler, F. & Gull, T. 1980, ApJ, 242, 294

Kerr, F.J., Bowers, P.F., Jackson, P.D. & Kerr, M. 1986, A&AS, 66, 373

Kouveliotou, C. et al. 1994, Nature, 368, 125

Kouveliotou, C. et al. 1998a, Nature, 393, 235

Kouveliotou, C., Kippen, M., Woods, P., Richardson, G., Connaughton, V. and McCollough, M. 1998b, IAU Circ. 6944

Kouveliotou, C., Strohmayer, T., Hurley, K., van Paradijs, J., Finger, M.H., Dieters, S., Woods, P., Thompson, C. & Duncan, R.C. 1999, ApJ, 510, L115

Kulkarni, S. R., Frail, D. A., Kassim, N. E., Murakami, T. & Vasisht, G. 1994, Nature, 368, 129

Mezger, P.G., Wilson, T.L., Gardner, F.F. & Milne, D.K. 1970, A&A, 4, 96

Murakami, T., Tanaka, Y., Kulkarni, S.R., Ogasaka, Y., Sonobe, T., Ogawara, Y., Aoki, T. & Yoshida, A. 1994, Nature, 368, 127

Murakami, T., Kubo, S., Shibazaki, N., Takeshima, T., Yoshida, A. & Kawai, N. 1999, ApJ, 510, L119

Predehl, P. & Schmitt, J.H.M.M. 1995, A&A, 293, 889

Rohlfs, K. & Wilson, T.L. 1996, *Tools of Radio Astronomy*, (Springer–Verlag).

Sarma, A.P., Goss, W.M., Green, A.J. & Frail, D.A. 1997, ApJ, 483, 335

Smith, D.A., Bradt, H.V. & Levine, A.M. 1999, ApJ, 519, L147

Solomon, P.M., Rivolo, A.R., Barrett, J.W. & Yahil, A. 1987, ApJ, 319, 730

Solomon, P. M. & Barrett, J. W. 1991, IAU Symp. 146, Dynamics of Galaxies and their Molecular Cloud Distributions, eds. F. Combes & F. Casoli, (Dordrecht: Kluwer), 235

Sonobe, T., Murakami, T., Kulkarni, S. R., Aoki, T. & Yoshida, A. 1994, ApJ, 436, L23

Strong, A.W. & Mattox, J.R. 1996, A&A, 308, L21

Thompson, C. & Duncan, R. C. 1995, MNRAS, 275, 255

Whiteoak, J.B.Z. & Green, A.J. 1996, A&AS, 118, 329

Woods, P.M., Kippen, M., van Paradijs, J., Kouveliotou, C. & Hurley, IAU Circ. 6948

Woods, P.M., Kouveliotou, C., van Paradijs, J., Finger, M.H. & Thompson, C. 1999a, ApJ, 518, L103

Woods, P.M., Kouveliotou, C., van Paradijs, J., Hurley, K., Kippen, R.M., Finger, M.H., Briggs, M.S., Dieters, S. & Fishman, G.J. 1999b, ApJ, 519, L139

This manuscript was prepared with the AAS LATEX macros v4.0.

Fig. 1.— ^{12}CO(J=2–1) spectrum toward SGR 1627–41. The different molecular clouds are labeled. The dotted line represents the HI spectrum at l=337.°0 and b=-0.°125 (intensity divided by 4.5). Positive velocities HI emission arises from gas beyond the solar circle. Antenna temperature have been converted into main beam brightness temperature.

Fig. 2.— Map of the CO emission, integrated between the velocities –80 and –40 km s^{-1}, from the survey of Bronfman et al. (1989). The CO gray levels are spaced at 12 K km s^{-1}, starting at 30 K km s^{-1}. Two GMCs are detected with central velocities of –71 (MC–71) and –56 km s^{-1} (MC–56). Contours indicate radio continuum emission at 4850 MHz (Condon et al. 1994), starting at 2.4 Jy beam^{-1} and spaced by 2.4 Jy beam^{-1}. The positions of the persistent X-ray counterpart to SGR 1627–41, the SNR G 337.0–0.1 and the H II regions G 337.1–0.2 and G 336.8+0.0 are indicated.

Table 1. Derived parameters from the $^{12}CO(J{=}1–0)$ and $^{12}CO(J{=}2–1)$ spectra for each of the molecular clouds along the line of sight to SGR 1627–41.

Name	V_{lsr} (km s^{-1})	ΔV(FWHM) (km s^{-1})	Near Distance (kpc)	Far Distance (kpc)	Estimated Distance (kpc)
MC–122	-121.5	4.6	6.7	9.0	*
MC–117	-116.6	5.5	6.4	9.2	*
MC–110	-110.3	4.0	6.1	9.5	*
MC–97	-96.5	4.0	5.6	10.1	*
MC–83	-83.3	5.0	5.1	10.6	*
MC–71	-70.9	11.0	4.6	11.0	11.0
MC–41	-40.6	7.0	3.1	12.5	3.1
MC–32	-32.2	5.7	2.6	13.0	2.6

Note. — * We did not attempt to resolve the distance ambiguity for MC-122, MC–117, MC–110, MC–97 and MC–83, since they are in front of MC–71 in either case.

Table 2. Contribution to the molecular hydrogen column density and to the optical extinction of each of the molecular clouds along the line of sight to SGR 1627–41.

Name	W(CO) (K km s^{-1})	$N(H_2)$ (10^{21} cm^{-2})	A_v (mag.)
MC–122	32.9 ± 3.3	6.3 ± 0.9	7.0 ± 1.1
MC–117	29.0 ± 2.9	5.5 ± 0.8	6.2 ± 0.9
MC–110	11.0 ± 1.1	2.1 ± 0.3	2.3 ± 0.4
MC–97	6.1 ± 1.2	1.2 ± 0.2	1.3 ± 0.3
MC–83	28.3 ± 2.9	5.4 ± 0.8	6.0 ± 0.9
MC–71	187.1± 14.0	35.5± 3.6	39.7± 4.0
MC–41	20.3 ± 2.0	3.9 ± 0.6	4.3 ± 0.6
MC–32	13.6 ± 1.4	2.6 ± 0.4	2.9 ± 0.4

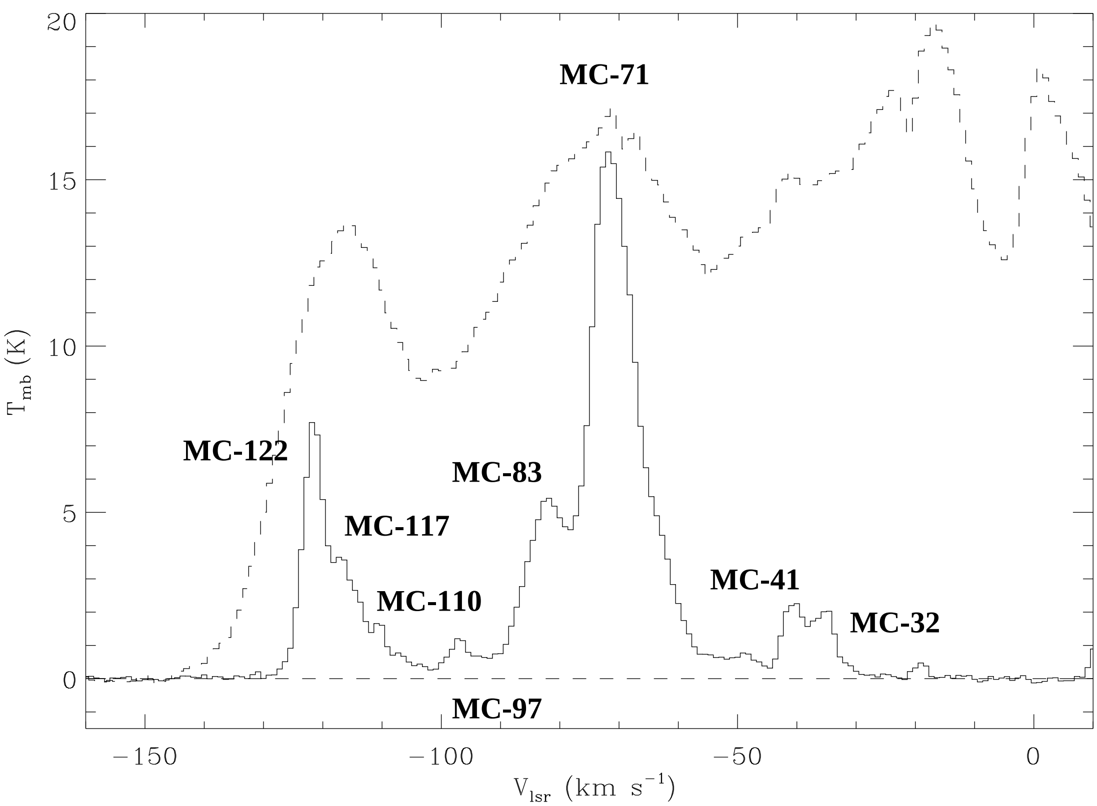
MC-71
MC-122
MC-83
MC-117
MC-110
MC-41
MC-32
MC-97
20
15
10
5
0
T_{mb} (K)
−150
−100
−50
0
V_{lsr} (km s^{-1})

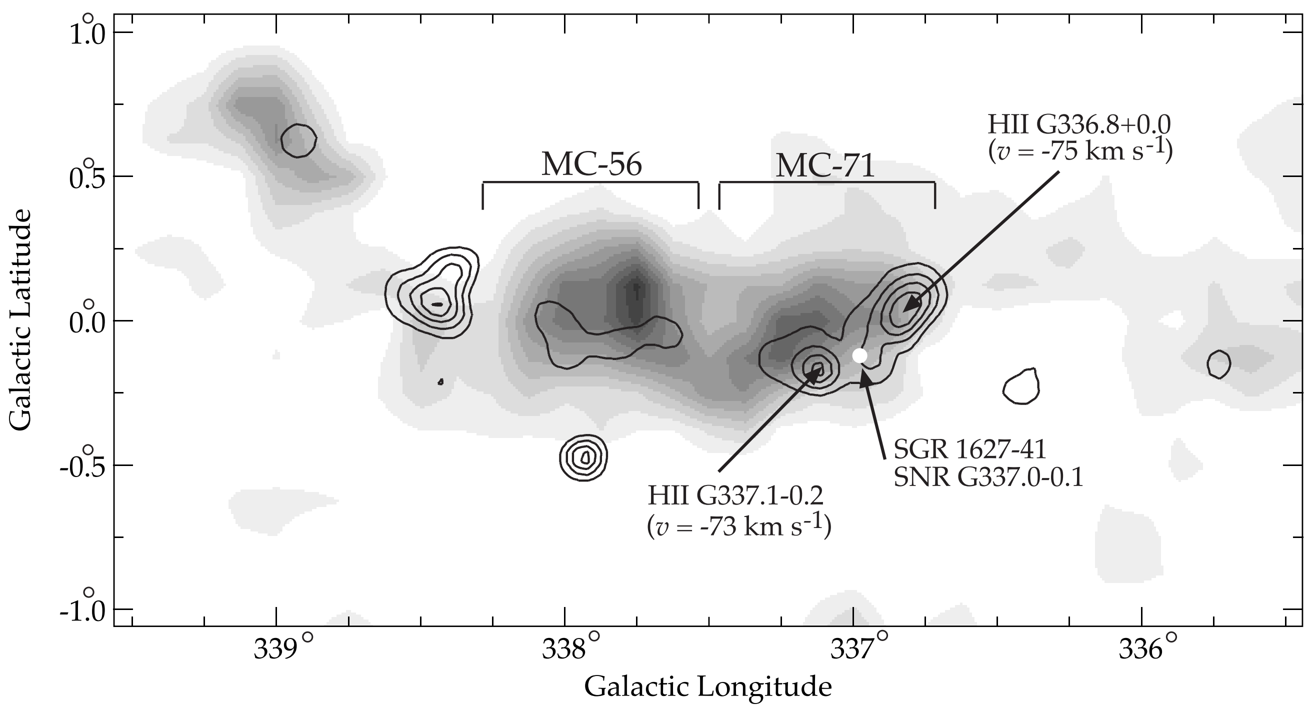
MC-56
MC-71
HII G336.8+0.0
(v = -75 km s-1)
HII G337.1-0.2
(v = -73 km s-1)
SGR 1627-41
SNR G337.0-0.1
Galactic Latitude
Galactic Longitude
1.0°
0.5°
0.0°
-0.5°
-1.0°
339°
338°
337°
336°